Research Article | Vol. 25, No. 7 | 3 Apr 2017 | OPTICS EXPRESS 8108

Optics EXPRESS

Magnetic field sensor of enhanced sensitivity and temperature self-calibration based on silica fiber Fabry-Perot resonator with silicone cavity

BIN ZHOU,[1,2,*] CHANGTAO LU,[1] BAREREM-MELGUEBA MAO,[1,3] HWA-YAW TAM,[2] AND SAILING HE[1]

[1]*South China Academy of Advanced Optoelectronics, South China Normal University, Guangzhou 510631, China*
[2]*Department of Electronic Engineering, The Hong Kong Polytechnic University, Kowloon, Hong Kong, China*
[3]*Centre Informatique et de Calcul, Universite de Lome, Togo*
[*]*zhoubin_mail@163.com*

Abstract: In this paper, a magnetic field sensor with enhanced sensitivity based on a fiber Fabry-Perot (F-P) cavity formed by a pair of identical fiber Bragg gratings (FBGs) is demonstrated. The F-P cavity which was filled with silicone rubber was bonded to a magnetic alloy at two positions such that when longitudinal strain is applied, the cavity is lengthened while the FBGs was virtually strain-free, effectively magnified the magnetic-field induced strain of the magnetic alloy. The FBGs could also be used for temperature-compensation because the FBG spectrum change is negligible compared to the F-P spectrum.

OCIS codes: (050.2230) Fabry-Perot; (060.3735) Fiber Bragg gratings; (060.2370) Fiber optics sensors.

References and links

1. P. Niewczas and J. R. McDonald, "Advanced optical sensors for power and energy systems applications," IEEE Trans. Instrum. Meas. **10**(1), 18–28 (2007).
2. L. Sun, S. Jiang, and J. R. Marciante, "All-fiber optical magnetic-field sensor based on Faraday rotation in highly terbium-doped fiber," Opt. Express **18**(6), 5407–5412 (2010).
3. M. Deng, D. Liu, W. Huang, and T. Zhu, "Highly-sensitive magnetic field sensor based on fiber ring laser," Opt. Express **24**(1), 645–651 (2016).
4. G. M. Müller, X. Gu, L. Yang, A. Frank, and K. Bohnert, "Inherent temperature compensation of fiber-optic current sensors employing spun highly birefringent fiber," Opt. Express **24**(10), 11164–11173 (2016).
5. J. Du, Y. Tao, Y. Liu, L. Ma, W. Zhang, and Z. He, "Highly sensitive and reconfigurable fiber optic current sensor by optical recirculating in a fiber loop," Opt. Express **24**(16), 17980–17988 (2016).
6. X. Zeng, H. Yang, Z. Wu, M. Song, Y. Lu, C. Yin, and Q. Xia, "Research on Current Sensor Based on POTDR," in *Asia-Pacific Optical Sensors Conference*, (Optical Society of America, 2016), paper JF2A.2.
7. F. Calkins, A. B. Flatau, and M. J. Dapino, "Overview of magnetostrictive sensor technology," J. Intell. Mater. Syst. Struct. **18**(10), 1057–1066 (2007).
8. C. Ambrosino, P. Capoluongo, S. Campopiano, A. Cutolo, M. Giordano, D. Davino, C. Visone, and A. Cusano, "Fiber bragg grating and magnetic shape memory alloy: Novel high-sensitivity magnetic Sensor," IEEE Sens. J. **7**(2), 228–229 (2007).
9. D. Davino, C. Visone, C. Ambrosino, S. Campopiano, A. Cusano, and A. Cutolo, "Compensation of hysteresis in magnetic field sensors employing Fiber Bragg Grating and magneto-elastic materials," Sens. Actuators A Phys. **147**(1), 127–136 (2008).
10. H. Liu, S. W. Or, and H. Y. Tam, "Magnetostrictive composite–fiber Bragg grating (MC–FBG) magnetic field sensor," Sens. Actuators A Phys. **173**(1), 122–126 (2012).
11. S. M. Quintero, A. M. Braga, H. I. Weber, A. C. Bruno, and J. F. Araújo, "A magnetostrictive composite-fiber Bragg Grating sensor," Sensors (Basel) **10**(9), 8119–8128 (2010).
12. M. Yang, J. Dai, C. Zhou, and D. Jiang, "Optical fiber magnetic field sensors with TbDyFe magnetostrictive thin films as sensing materials," Opt. Express **17**(23), 20777–20782 (2009).
13. Q. Zhao, Y. Dai, T. Li, B. Liu, M. Yang, and G. Yin, "Femtosecond laser ablation of microstructures in fiber and application in magnetic field sensing," Opt. Lett. **39**(7), 1905–1908 (2014).

#286419 https://doi.org/10.1364/OE.25.008108
Journal © 2017 Received 9 Feb 2017; revised 24 Mar 2017; accepted 24 Mar 2017; published 29 Mar 2017

Optics EXPRESS

14. J. Nascimento, J. M. Baptista, P. A. S. Jorge, J. L. Cruz, and M. V. Andrés, "Passive interferometric interrogation of a magnetic field sensor using an erbium doped fiber optic laser with magnetostrictive transducer," Sens. Actuators A Phys. **235**, 227–233 (2015).
15. F. Chen, Y. Jiang, and L. Jiang, "3 × 3 coupler based interferometric magnetic field sensor using a TbDyFe rod," Appl. Opt. **54**(8), 2085–2090 (2015).
16. J. M. Jani, M. Leary, A. Subic, and M. A. Gibson, "A review of shape memory alloy research, applications and opportunities," Mater. Des. **56**, 1078–1113 (2014).
17. J. Tellinen, I. Suorsa, A. Jääskeläinen, I. Aaltio, and K. Ullakko, "Basic properties of magnetic shape memory actuators," In *8th International Conference Actuator*, (2002) pp. 566–569.
18. Y. Liu, K. S. Chiang, and P. L. Chu, "Multiplexing of temperature-compensated fiber-Bragg-grating magnetostrictive sensors with a dual-wavelength pulse laser," IEEE Photonics Technol. Lett. **16**(2), 572–574 (2004).
19. G. N. Smith, T. Allsop, K. Kalli, C. Koutsides, R. Neal, K. Sugden, P. Culverhouse, and I. Bennion, "Characterisation and performance of a Terfenol-D coated femtosecond laser inscribed optical fibre Bragg sensor with a laser ablated microslot for the detection of static magnetic fields," Opt. Express **19**(1), 363–370 (2011).
20. F. Chen, Y. Jiang, H. Gao, and L. Jiang, "A high-finesse fiber optic Fabry–Perot interferometer based magnetic-field sensor," Opt. Laser Technol. **71**, 62–65 (2015).
21. D. Fuard, T. Tzvetkova-Chevolleau, S. Decossas, P. Tracqui, and P. Schiavone, "Optimization of poly-di-methyl-siloxane (PDMS) substrates for studying cellular adhesion and motility," Microelectron. Eng. **85**(5-6), 1289–1293 (2008).
22. T. Ioppolo, U. Ayaz, and M. Ötügen, "High-resolution force sensor based on morphology dependent optical resonances of polymeric spheres," J. Appl. Phys. **105**(1), 013535 (2009).
23. A. D. Kersey, M. A. Davis, H. J. Patrick, M. LeBlanc, K. Koo, C. Askins, M. Putnam, and E. J. Friebele, "Fiber grating sensors," J. Lightwave Technol. **15**(8), 1442–1463 (1997).
24. B. Zhou, H. Jiang, R. Wang, and C. Lu, "Optical fiber Fabry–Perot filter with tunable cavity for high-precision resonance wavelength adjustment," J. Lightwave Technol. **33**(14), 2950–2954 (2015).
25. Y. O. Barmenkov, D. Zalvidea, S. Torres-Peiró, J. L. Cruz, and M. V. Andrés, "Effective length of short Fabry-Perot cavity formed by uniform fiber Bragg gratings," Opt. Express **14**(14), 6394–6399 (2006).
26. W. F. Yeung and A. R. Johnston, "Effect of temperature on optical fiber transmission," Appl. Opt. **17**(23), 3703–3705 (1978).

1. Introduction

With the help of Faraday effect [1,2] and functional packaging, optical fiber magnetic sensor has become one of the promising devices in the measurement of magnetic fields and electric current. However, Faraday effect based sensors require long length of optical fiber [1] to generate a detectable Faraday rotation or employed special material (e.g. terbium) doped fiber to enlarge the Verdet coefficient [2] so as to shorten the sensing fiber. In recent years several technologies have been developed to enhance the performances of optical fiber current and magnetic sensors [3–6], with better sensitivity [3], temperature-compensation [4], reconfigurable feature, larger signal to noise ratio (SNR) [5], and distributed magnetic field and current sensing capabilities [6]. Magnetostriction is a property of ferromagnetic materials that change shapes during magnetization [7]. Magnetostrictive materials are the most popular material used to fabricate optic fiber magnetic field sensors by directly bonding an FBG onto a magnetostrictive bar [8–11], coating an FBG with magnetostrictive film [12,13], or using magnetostrictive materials to change the optical path length of optical fiber Mach–Zehnder interferometers [14,15]. These magnetic sensors are gradually being used in the scientific research and industry areas. However most of them still suffer two deficiencies: one is the low sensitivity, because the magnetic-field induced strain of most magnetostrictive materials is very small, usually less than several ppm/mT, and although giant magnetostrictive materials are available and the total strain at saturation magnetic field can reach 10%, their sensitivities are still limited to ~100 ppm/mT [8,16,17]; the other issue is temperature crosstalk, which requires external temperature-compensated sensors [18] or temperature self-calibration technologies [19,20].

In this paper, we addressed the issues of low sensitivity of magnetostrictive material packaged fiber sensor, and temperature crosstalk. We proposed the use of a Fabry-Perot cavity formed by two identical FBGs to magnify the magnetic-field induced strain of a magnetic alloy. The sensor's structure was well designed, and a silica/silicone/silica

Optics EXPRESS

composite Fabry-Perot (F-P) cavity was applied to enhance the sensitivity. The fiber magnetic sensor can achieve high magnetic-field sensitivity even with magnetic materials of very small magnetostriction. In addition, the FBGs are insensitive to magnetic-field and thus could be used for temperature-compensation.

2. Magnetic field sensor design and fabrication

Figure 1 shows the design of the proposed optical fiber magnetic-field sensor and the experimental setup. The magnetic-field sensor was constructed by sandwiching a thin layer of transparent silicone rubber between two FBGs with identical Bragg wavelength to create a F-P cavity. The silicone helps to keep the optical alignment between the two FBGs. As the Young's modulus and Poisson's ratio of the silicone are much smaller than silica, when longitudinal strain is applied, the silicone is lengthened while the FBGs are virtually strain-free. This arrangement effectively magnified the magnetic-field induced strain of the magnetic rod on which the F-P cavity is bonded. The sensitivity enhancement and the self-calibration properties are realized at the same time by using the F-P resonant wavelength as sensor and the FBG Bragg wavelength as reference.

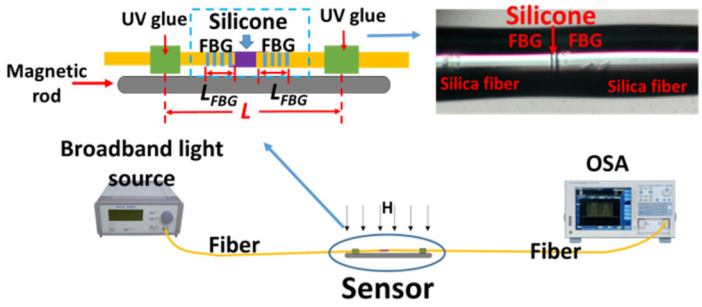

Fig. 1. Sensor structure and experimental setup. The left inset is the detailed structure of the fiber F-P interferometer, which is fixed to a magnetostrictive rod on two ends. The right inset is the microscope image of the sensitivity enhanced F-P resonator with silicone filled cavity. OSA: optical spectrum analyzer.

This magnetic alloy has high saturation flux density (2.4 T) and very low magnetic field sensitivity. It is not sufficient for small magnetic field measurement and is only suitable for large dynamic range sensing. However, with the help of the proposed sensitivity enhanced F-P resonator, its performance can be greatly improved, and this low-cost magnetic alloy is capable for small magnetic field measurement. The experimental results shows that the sensitivity of this composited sensor is even higher than the giant magnetostrictive materials based FBG sensors that have been reported, such as magnetic shape memory alloy [8] and Terfenol-D [10,11] composited sensors.

The fabrication processes of the proposed highly sensitive magnetic sensor are as follows: 1. Inscribe a uniform FBG (grating length: 3 mm) on a hydrogen-loaded single mode fiber with phase mask technology; 2. Cut the uniform FBG into two equal segments; 3. Manually align and soft splice the two identical FBGs with a small drop of silicone glue (PDMS, Dowcorning Ltd., model: Sylgard 184, mixed weight ratio: 10:1) to form an F-P cavity; 4. Stretch the F-P cavity gently to produce the pre-stress and bond it to the magnetostrictive rod from two ends with UV glue.

The fabricated magnetic sensor and experimental setup are shown in Fig. 1. The left inset is the detailed structure of the magnetic sensor and the right inset is the microscope image of the sensitivity enhanced F-P cavity in which the silicone filled cavity is shown. The physical length of the FBGs, the physical length of the FP cavity at zero magnetic field intensity, and the total physical length of the sensor (L in the left inset of Fig. 1) are 1.5 mm, 15 μm and 45 mm, respectively. To demonstrate the sensitivity enhancement, a reference FBG was bonded

Optics EXPRESS

directly onto the magnetic rod using a UV glue to measure the magnetic-field induced strain of the magnetic rod.

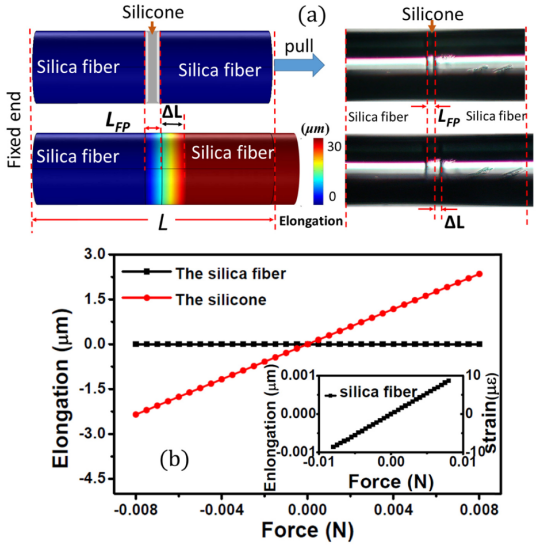

Fig. 2. Elongation of the F-P resonator with silica/silicone/silica structure with applying axial force. (a) The simulated diagrams (left) and the microscope images (right) of F-P resonator with (bottom) and without (top) axial force. The color bar shows the lengthening at fiber axis direction. (b) The simulation elongation of the silica fiber and silicone cavity. The inset shows the zoomed in elongation and strain of the silica fiber.

The lengthening of the silicone cavity and the silica fiber are studied using the simulation software COMSOL (3D structural mechanics model). The structure parameters in the simulation are the same as described in Fig. 1. The Young's modulus of silica fiber and silicone cavity here are 73 GPa and 4.18 MPa, and the Poisson's ratio of silica and silicone are 0.167 and 0.034 respectively, which are the typical values reported [21]. The difference in the Young's modulus between these two materials is so large, that, when the F-P interferometer is pulled at axis direction, most of the lengthening happens at silicone cavity, and most of the force is absorbed by the silicone, leading to virtually strain-free in the silica fiber. Figure 2(a) shows the simulated and tested deformation when pulling the F-P resonator. The color bar shows the lengthening at fiber axis direction. Figure 2(b) shows that the elongation of the silica fiber is nearly negligible compared to silicone, and the inset of Fig. 2(b) shows that the strain in the silicone area is about 25000 times larger than that of silica fiber under the same stress. There are two important conclusions from the above analysis: 1. The sensitivity of the F-P spectrum to the stress is enhanced, as virtually all the elongation occurred in the silicone. 2. The FBG inscribed on the silica fiber is insensitive to the stress and can be used as temperature-compensation.

In the experimental setup the fiber sensor is glued to the magnetic rod at its two ends. After applying magnetic field, the length of the magnetic rod changes and its magnetic-field induced strain is $\Delta L / L$, where ΔL and L are defined in Fig. 1 and Fig. 2(a). When the silica fiber is pulled, the contribution of the photoelastic effect to the optical path length change in the fiber is comparable to the physical elongation, while on the contrary, the contribution of the photoelastic effect to the optical path length change is negligible in the silicone compared to the physical elongation [22,23]. The normalized wavelength shift $\Delta\lambda / \lambda$ of an FBG directly glued onto the magnetic rod would thus be $(1-P_e)\Delta L / L$ [10,23], where P_e is the photoelastic coefficient of silica and its typical value is 0.22.

Optics EXPRESS

To describe the sensitivity enhancement of the proposed structure, here we define the enhancement A as: the ratio between normalized wavelength shifts of the F-P structure and the FBG directly glued to the magnetic alloy. In the proposed fiber sensor, most of the deformation occurred in the silicone, so the sensitivity is enhanced by:

$$A = \frac{n_{silicone}\Delta L / L_{eff\_FP}}{(1-P_\varepsilon)\Delta L / L} = \frac{n_{silicone} L}{(1-P_\varepsilon) L_{eff\_FP}}, \tag{1}$$

where $n_{silicone}$ is the reflective index of silicone which changes a little while being stretched [20], L_{eff_FP} is the effective optical cavity length of the F-P resonator, which is much shorter than L, thus the sensitivity can be enhanced greatly. It should be mentioned that the F-P resonator is formed by two FBGs that work as the reflectors, and as the grating length is not negligible, the cavity optical path length L_{eff_FP} not only includes the silicone area, but also includes some part of the FBG [24,25].

$$L_{eff\_FP} = n_{silicone} L + 2L_{eff\_FBG}, \tag{2}$$

where $n_{silicone}$ and $L_{silicone}$ are the reflective index and the physical length of the silicone. L_{eff_FBG} is the effective optical path length of the FBGs which is defined as:

$$L_{eff\_FBG} = n_{silica} L_{FBG} \frac{\sqrt{R}}{2atanh\sqrt{R}}, \tag{3}$$

where $n_{silicone}$, L_{FBG} and R are the reflective index, physical length and reflectivity of the FBG. In the experiment, L_{FBG} and $L_{silicone}$ are 1.5 mm and 15 μm, respectively. n_{silica} and $n_{silicone}$ are 1.445 and 1.41, which are the typical values around room temperature [26]. The reflectivity of the FBG is 12 dB. The length of the magnetic alloy L is 45 mm. So L_{eff_FP} is 1.04 mm and the sensitivity enhancement is estimated to be 78 times, i.e., 18.9 dB.

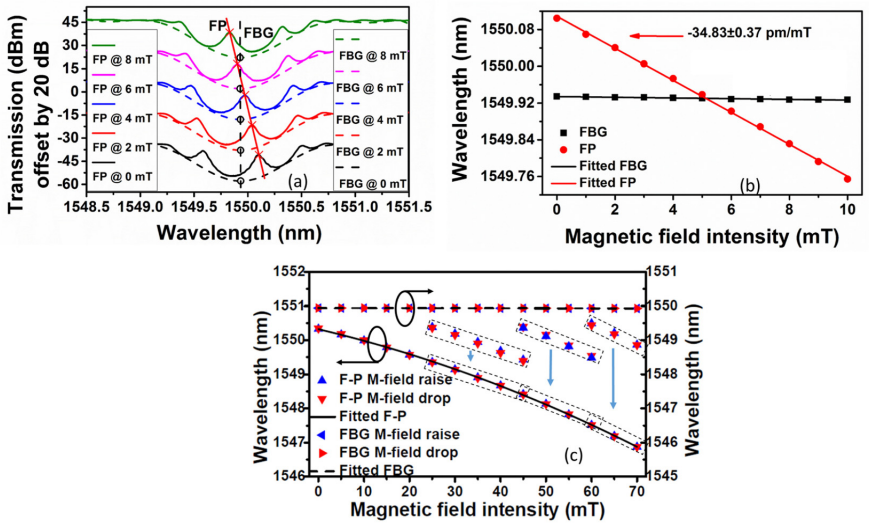

Fig. 3. (a) The transmission spectrum of F-P cavity (solid line) and its fitted envelope, i.e. the FBG spectrum (dashed line) shift with the increasing magnetic field. The 20 dB offset is for graphic clarity. (b) One of the F-P peak wavelength and the FBG Bragg wavelength vary at different magnetic field. (c) Large scale and repeatability testing. Negligible hysteresis effect observed as the soft magnetostrictive alloy applied.

Optics EXPRESS

3. Experiment and sensitivity enhancement analysis

An iron cobalt vanadium supermendur alloy (Hongwon, Ltd, China, model: 1j22) was used in our experiment. The magnetic alloy has high saturation flux density (2.4 T) and very low sensitivity of less than 100 με even at the saturation magnetic field, and it is too insensitive to measure magnetic field directly. The proposed sensitivity enhanced F-P structure was glued onto the magnetic alloy as shown in Fig. 1 to make it possible to measure small magnetic field. Figure 3 shows the transmission spectra of the F-P sensor and the FBG at different magnetic field intensities. The 20 dB offset between each spectrum is for graphic clarity. The FBG spectrum is recovered by fitting the envelope of the F-P spectrum. The envelope curves (dashed lines in Fig. 3(a)) are actually polynomials fitted from the F-P spectra and then multiplied by a suitable coefficient. The silicone rubber in the F-P resonator was pre-stressed prior gluing onto the magnetic alloy, The resonance peaks of F-P cavity decreases linearly with magnetic field (sensitivity: −34.83 ± 0.37 pm/mT) while the recovered FBG Bragg wavelength remains almost unchanged.

The sensitivity of the proposed sensor is so large that its dynamic range is limited by the FBG bandwidth. In order to enlarge its measurement range, multi resonant peaks are used as shown in Fig. 3(c). The FBG spectrum shift is 1 nm offset from the F-P spectrum and shown at right axis for graphic clarity. The response of the F-P and recovered FBG spectra are recorded and shown in Fig. 3(c) when the magnetic field was increased to 70 mT and decreased to 0 mT. The iron cobalt vanadium supermendur magnetic alloy used here is a soft magnetic material, and its small magnetic hysteresis effect is due to the fact that it is operating far from the saturation region of ~2400 mT. The repeatability during magnetization and demagnetization processes shown in Fig. 3(c) is very good. The magnetic hysteresis effect is always a troublesome problem for sensing. The negligible hysteresis property makes the sensor magnetization path insensitive and able to work at any complicated varying magnetic field.

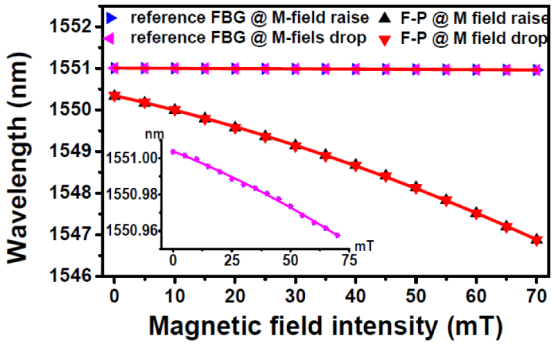

Fig. 4. The tested wavelength shifts to the magnetic field when the F-P sensor and an extra reference FBG glued together to the magnetic alloy. The inset shown the FBG response. The result demonstrates the large sensitivity enhancement of the soft cavity F-P structure.

In order to specify the exact value of the sensitivity enhancement of the silicone cavity F-P senor, an extra FBG is glued directly onto the magnetic alloy. Figure 4 shows the wavelength response of the F-P and the extra reference FBG. The inset is the wavelength change of the extra reference FBG and from which the enhancement is calculated to be 18.7 dB (the wavelength changes are 3.472 nm and 0.046 nm respectively), and this result matches the theoretical estimation value mentioned earlier.

In order to demonstrate the temperature self-calibration capability, the sensor was heated and the F-P spectrum was recoded. Figure 5(a) shows the F-P spectra and their fitted envelope, i.e. the FBG spectra when temperature increases from 30 °C to 34 °C, and Fig. 5(b) shows the F-P resonant wavelength and the recovered FBG Bragg wavelength shifts. Their

Optics EXPRESS

linear fitting coefficients are 255.75 ± 2.27 pm/°C and 10.31 ± 0.40 pm/°C, respectively. The high temperature coefficient of the F-P cavity is from the relatively high thermal expansion coefficient of the magnetic alloy and silicone. The sensitivity enhancement structure not only enhances the magnetic sensitivity of the alloy but also enhances temperature sensitivity. So it is important to calibrate the temperature induced wavelength change of the F-P cavity. The tested FBG temperature coefficient is the typical value of an FBG fabricated on a single mode silica fiber [19], so the influence of the thermal expansion of the magnetic alloy to the FBG is negligible. Thus, it indicates that the recovered FBG spectrum can be used for the temperature-compensation.

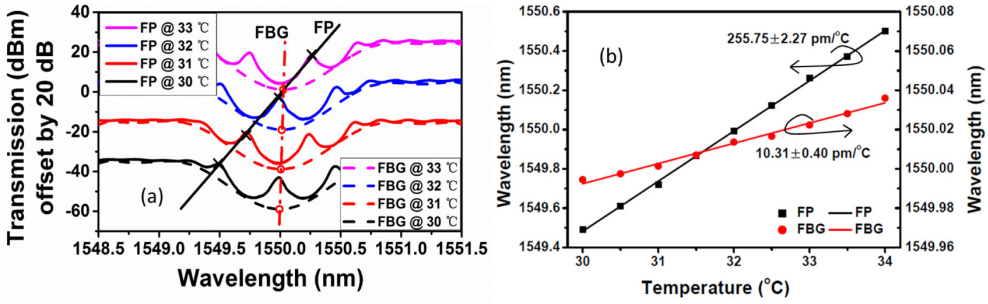

Fig. 5. (a) The transmission spectrum of F-P cavity (solid line) and its fitted envelope, i.e. the FBG spectrum (dashed line) shift with the increasing temperature at zero magnetic strength. The 20 dB offset is for graphic clarity. (b) One of the F-P peak wavelength and the FBG Bragg wavelengths vary at different temperature.

4. Summary

We propose a magnetic field sensor with enhanced sensitivity, temperature self-calibration capability, and negligible hysteresis effect. The sensitivity enhancement was measured to be 18.7 dB which is in excellent agreement with the predicted result. The recovered FBG spectrum used for temperature-compensation, is influenced slightly by the stress and thermal expansion of the magnetic alloy. Soft magnetic alloy with high saturation flux density of 2.4T was used. Operating the sensor far from the saturation flux density significantly reduced the troublesome magnetic hysteresis effect, which makes the sensor magnetization path insensitive and able to work at any complicated varying magnetic field. The proposed sensor using inexpensive magnetic alloy and simple structure is a good candidate for magnetic and current sensing.

Funding

The Hong Kong Scholars Program (XJ2014027); National Natural Science Foundation of China (NSFC) (61307053); China Postdoctoral Science Foundation (2016M590794).

Acknowledgments

This study was supported by the Joint International Research Laboratory of Optical Information.